HHS Public Access

Author manuscript

Clin Immunol. Author manuscript; available in PMC 2024 March 01.

Published in final edited form as:

Clin Immunol. 2023 March ; 248: 109213. doi:10.1016/j.clim.2022.109213.

Kidney tubular epithelial cell ferroptosis links glomerular injury to tubulointerstitial pathology in lupus nephritis

Abdel A Alli[1,*], **Dhruv Desai**[2,*], **Ahmed Elshika**[3], **Marcus Conrad**[4], **Bettina Proneth**[4], **William Clapp**[3], **Carl Atkinson**[2], **Mark Segal**[2], **Louis A. Searcy**[5], **Nancy D. Denslow**[5], **Subhashini Bolisetty**[6], **Borna Mehrad**[2], **Laurence Morel**[3], **Yogesh Scindia**[2,3,#]

[1]Department of Physiology and Aging, University of Florida, Gainesville, USA

[2]Department of Medicine, University of Florida, Gainesville, USA

[3]Department of Pathology, Immunology and Laboratory Medicine, University of Florida, Gainesville, USA

[4]Institute of Metabolism and Cell Death, Helmholtz Zentrum Munich, Germany

[5]Department of Physiological Sciences and Center for Environmental and Human Toxicology

[6]Department of Medicine, University of Alabama, Birmingham, USA

Abstract

Ferroptosis is a druggable, iron-dependent form of cell death that is characterized by lipid peroxidation but has received little attention in lupus nephritis. Kidneys of lupus nephritis patients and mice showed increased lipid peroxidation mainly in the tubular segments and an increase in Acyl-CoA synthetase long-chain family member 4, a pro-ferroptosis enzyme. Nephritic mice had an attenuated expression of SLC7A11, a cystine importer, an impaired glutathione synthesis pathway, and low expression of glutathione peroxidase 4, a ferroptosis inhibitor. Lipidomics of nephritic kidneys confirmed ferroptosis. Using nephrotoxic serum, we induced immune complex glomerulonephritis in congenic mice and demonstrate that impaired iron sequestration within the proximal tubules exacerbates ferroptosis. Lupus nephritis patient serum rendered human proximal tubular cells susceptibility to ferroptosis which was inhibited by Liproxstatin-2, a novel ferroptosis inhibitor. Collectively, our findings identify intra-renal ferroptosis as a pathological feature and contributor to tubular injury in human and murine lupus nephritis.

[#]Corresponding author: Yogesh Scindia, PhD, Departments of Medicine and Pathology, The University of Florida, Phone: 352-294-8823, Fax: 352-273-9154, yogesh.scindia@medicine.ufl.edu.

[*]Abdel Alli and Dhruv Desai contributed equally to this work

Author Contribution

YS conceptualized the work and wrote the original draft. AAA, DD, AE, and YS did most of the experiments. AA, LAS, and NDD performed lipidomics and mass spectrometric studies. WC and CA scored the kidney pathology. LM generated the (NZW X BXSB) F1 mice and helped in measuring clinical parameters of disease, and BM provided input for iron biology. BP and MC provided Liproxstatin-2 and helped design the in-vitro studies. MS helped with the patient studies. SB helped generate the *FtH*$^{PT-/-}$ mice. All authors helped edit and approved the final version of the manuscript.

Conflict of interest and Disclosures: None

The authors have declared that no conflict of interest exists

Keywords

Ferroptosis; Iron; Lupus nephritis; SLE; Liproxstatin; GPX4; ACSL4

1. Introduction.

Nephritis complicates the course of about 50% of the patients with systemic lupus erythematosus (SLE), resulting in increased morbidity and mortality [1–3]. With best available therapy, the rate of complete remission for proliferative kidney disease remains below 50% [4]. Lupus nephritis is thought to initiate in the glomeruli, but tubulointerstitial inflammation, fibrosis, and atrophy strongly correlate with renal dysfunction, independent of the extent of glomerular damage [5], and predict worse outcomes [6–8]. In this context, over-absorption of IgG anti-dsDNA antibodies and albumin by proximal tubular epithelial cells results in ROS-mediated tubular injury and interstitial inflammation [9, 10]. The mechanisms that lead to tubular epithelial cell injury following glomerular injury in lupus nephritis are, however, not well-defined.

Oxidative stress and ROS worsen human and animal SLE [11] and lupus nephritis [12]. Iron accumulates in the tubular segments of human [13] and mouse kidneys in lupus nephritis [14, 15], and plays a central role in generating ROS [16]. Multiple receptors on proximal tubular epithelial cells import iron [13] increasing their susceptibility to iron-mediated pathology following the loss of glomerular permeability. We, and others, have demonstrated that pharmacological inhibition of kidney iron accumulation mitigates proximal tubular epithelial cell injury and kidney failure in lupus nephritis, even in the presence of anti-dsDNA antibodies and glomerular immune complexes [14, 17]. While these studies establish the role of iron and tubular cells in the pathogenesis of lupus nephritis, the underlying mechanisms by which iron induces this pathology remain poorly defined.

Bioavailable iron mediates the Fenton reaction to produce ROS [16]. While intracellular iron increases DNA hydroxymethylation level in lupus CD4+ T cells and overexpression of immune related genes [18], it also serves as a cofactor for lipoxygenases to catalyze polyunsaturated fatty acids (PUFA) peroxidation [19]. Ferroptosis is an iron-dependent form of regulated cell death identified by iron-catalyzed damage to the lipid membrane [20, 21]. Growing evidence has identified a central pathophysiological role for ferroptosis in kidney injury [22], nephron loss, and tubular necrosis [23]. Lipid peroxidation, the key feature of ferroptosis, is increased in lupus patients [24]. A recent study for the first-time implicated lupus serum in inducing neutrophil ferroptosis in lupus and showed that selective haploinsufficiency of the ferroptosis inhibitor glutathione peroxidase-4 (GPX4) in mouse neutrophils recapitulated features of human SLE [25]. This study identified that lupus serum factors like autoantibodies and type I IFNs cooperatively induce ferroptosis in neutrophils but not in lymphocytes and monocytes. Moreover, ferroptosis-related molecular markers were identified in the glomeruli and tubulointerstitium of lupus nephritis patients[26]. However, majority of the data is based on transcriptomics, not validated, and lacks evidence in animal models.

Herein, we identify ferroptosis and lipid peroxidation in human lupus nephritis biopsies and kidneys of two spontaneous murine lupus models. We highlight the importance of iron sequestration in kidney proximal tubules which was validated in vitro using human proximal renal tubular cell line and siRNA knockdown studies. Finally, we demonstrate that a novel, second-generation ferroptosis inhibitor Liproxstatin-2, reverses lupus nephritis patient (Class IV) serum-induced ferroptosis in human proximal tubular epithelial cells.

2. Materials and Methods

2.1 Approvals

Animal studies were approved by The Animal Care and Use Committee of the University of Florida, and human studies were performed per the Declaration of Helsinki, under protocols approved by the University of Florida Institutional Review Board (IRB#201601162 and IRB#201601170) after written informed consent was received from participants.

2.2 Mice

Female MRL/lpr, male *FtH*$^{fl/fl}$, and parental strains of (NZW X BXSB) F1 mice were purchased from the Jackson Laboratories (Bar Harbor, USA), and *Pepck*$^{Cre/wt}$ mice were gifts from Dr. Volker Haase (Vanderbilt University). The transgenic mice deficient in *FtH1* expression only in the kidney's proximal tubules (*FtH*$^{PT-/-}$) were generated as described in our previous studies [27, 28]. Animals were maintained on standard chow in SPF conditions. Tissue was collected from 4 and 16 week old (NZW X BXSB) F1 males and 8 and 20 week old female MRL/lpr mice.

2.3 Induction of nephrotoxic serum glomerulonephritis in mice

10–12 week old female *FtH*$^{PT-/-}$ and *FtHPT*$^{+/+}$ littermate control mice were preimmunized intraperitoneally with 200 μg of sheep IgG (Serotec) in Addavax (Invivogen), followed by intravenous injection of sheep nephrotoxic serum or normal donor sheep serum (2.5 μL of serum per gram of mouse, Probetex, San Antonia, Tx) 4 d later as described previously [29]. Tissue was collected 14 d later.

2.4 Biochemical assays, tissue samples, and histology

Proteinuria was assessed by adding 50 μL urine on Siemens Multistix 8 SG dipsticks. Ketamine (120 mg/kg)/xylazine (12 mg/kg) mix was used to anesthetize the mice. Blood was drawn from the axillary vein before euthanasia. Kidney slices were processesd for gene, protein and histology as described [17]. Paraffin-embedded or cryosections of human biopsies or mouse kidney sections (3 μm) were used for Acyl-CoA synthetase long-chain family member 4 (ACSL4), 4-hydroxynonenal (4-HNE), α smooth muscle actin (αSMA), F4/80+ macrophages, CD4+ T cells and immune complexes. Details of staining and antibodies is provided in the Supplemental Methods.

2.5 In vitro studies

HK-2 cells, a normal human proximal tubular cell line (ATCC) were used in this study. All experiments were carried out in a medium containing 5% serum from lupus nephritis

(Class IV) patients or healthy donors. For gene knockdown studies, silencer select siRNA for human FtH1 and negative control siRNA from ThermoFisher Scientific were used. Liproxstain-2 a proprietary new generation ferroptosis inhibitor by ROSCUE Therapeutics was used. Experimental details are provided in Supplemental Methods section.

2.6 Preparation of Kidney and Cell Extracts, and Western Blotting

Western blotting was performed as described in [17] and the Supplemental Methods section.

2.7 Detection of serum IgG, IgG2a, and anti-dsDNA antibodies.

Mouse serum IgG and IgG2a were detected using commercial ELISA kits (ThermoFisher) as per manufacturers' instructions. Anti-dsDNA IgG was measured in 1:100 diluted serum using plates coated with 50 μg/ml dsDNA as described [30].

2.8 RT-PCR

RNA isolation, cDNA synthesis and RT-PCR was performed as described in our previous publication [17], the details of which are provided in the Supplemental Methods section.

2.9 Lipid extraction and liquid chromatograhpy-mass spectrometry

Lipids were extracted with a modified Bligh-Dyer protocol [31]. The details of sample preparation and conditions for performing liquid chromatography-mass spectrometric analysis are provided in the Supplemental Methods section.

2.10 Statistics

Statistical significance was determined by applying a Mann-Whitney test for groups not passing the normality test. 1-way and 2-way analysis of variance (ANOVA) with Tukey`s or Holm-Šídák's multiple comparisons test were used to compare more than 2 groups of experimental conditions and represented as mean ± SEM. All analyses were performed using GraphPad Prism 9 (GraphPad Inc, San Diego, CA).

3. Results

3.1 Tubular injury is a prominent feature in lupus nephritis

We began by comparing young non-nephritic and nephritic MRL/lpr mice. Glomerular immune complexes were observed at 8 weeks (Figure 1A) but were associated with minimal proteinuria (Proteinuria: 8 weeks,10±6 mg/dL). However, intense glomerular and tubular immune complexes (Figure 1B, white arrows indicate tubular immune complexes) with severe proteinuria (Proteinuria: 20 weeks, 1775±147 mg/dL) were a feature in 20-week-old mice. There was no histological evidence of injury (Figure 1C, Supplemental Figure 1A) at 8 weeks. In comparison H&E staining showed a high degree of cellular infiltrates in periglomerular and tubulointerstitial regions (Figure 1D). Tubulointerstitial injury was a distinct and prominent feature in diseased kidneys. Multiple atrophic tubules with loss of brush border and enlarged basement membrane, blebbed tubules, and interstitial fibrosis were observed in nephritic kidneys (20-week-old, Figure 1D and Supplemental Figure 1B). Sensitive markers of proximal tubular injury, *Ngal* and *Kim1*, were not detected at

8 weeks but were significantly elevated at 20 weeks of age (Figure 1E–F). Immune cell infiltrates composed of macrophages (Supplemental Figure 1C–D), and CD4 T cells were also observed in the peritubular region of nephritic mice (Supplemental Figure 1E–F).

3.2 Iron accumulation signature in the kidneys of nephritic mice

Iron was not detected by Perl's staining in non-nephritic mice (Figure 2A). However, substantial iron deposits were observed in the tubular cells of nephritic mice (Figure 2B). Though severely injured, glomeruli were devoid of iron deposits. Kidney gene expression of *Zip8* and *Zip14*, which encode for SLC39A8 and SLC39A14, the metal transporters that mediate non-transferrin-bound iron uptake into proximal renal tubular cells [32], were significantly decreased in nephritic mice (Figure 2C–D). There was a concomitant increase in protein expression of ferritin heavy chain (FtH1) (Figure 2E–F). FtH1 sequesters iron for storage within its core [33, 34]. While FtH1 is exquisitely sensitive to cellular iron, it is independently regulated by inflammation [35]. Since glomerular injury and renal inflammation precede tubular injury in glomerulonephritis [36], it is possible that the observed increase in FtH1 may be driven in part by early intrarenal inflammation as well as by iron accumulation.

3.3 Lupus nephritis kidneys display oxidative stress and distinct ferroptosis signature

Ferroptosis is an iron-dependent form of oxidative injury primarily studied in acute tubular injury in the kidneys [22, 37, 38]. Compared to young non-nephritic MRL/lpr females, the kidneys of nephritic females had a higher gene expression of NAD(P)H Quinone Dehydrogenase 1 (*Nqo1*), heme oxygenase 1 (*Hmox1*), and downregulation of thioredoxin 1 (*Txnrd1*), the genes associated with protection against oxidative stress (Supplemental Figure 2A–C). Increased oxidative stress was associated with a ferroptosis gene signature (Supplemental Figure 2D–F).

SLC7A11 is responsible for cystine import into the cells [39], and cystine availability is the rate-limiting step in the biosynthesis of glutathione (GSH)[40]. We observed that SLC7A11 protein expression was significantly attenuated in nephritic MRL/lpr females (Figure 3A–B). After cysteine import, Glutamate cysteine ligase (GLC) catalyzes the ligation of glutamate and cysteine and as such is the rate-limiting enzyme in glutathione synthesis[41]. GLC comprises two independent gene products, the glutamate-cysteine ligase-catalytic (*Gclc*) and glutamate-cysteine ligase-modifier (*Gclm*) subunits. We found lower gene expression of both *Gclc* and *Gclm* in nephritic MRL/lpr females (Figure 3C–D), indicating low levels of reduced glutathione. In support, the expression of GPX4, a glutathione-dependent ferroptosis inhibitor[42], was significantly attenuated in nephritic mice (Figure 3E–F). Nephritic mice also had an elevated expression of Acyl-CoA synthetase long-chain family member 4 (ACSL4), an essential component for the execution of ferroptosis[43] (Figure 4A–B). ACSL4 dictates the sensitivity to ferroptosis by altering the cells lipid composition[43]. Additionally, nephritic kidneys had a higher immunoreactivity to 4-hydroxynonenal (4-HNE), an established lipid peroxidation marker (Figure4C–D). 4-HNE immunoreactivity was primarily observed in the kidney tubules, a region of iron accumulation (Figure 2B).

3.4 Lipidomics identifies a distinct profile and pattern in nephritic kidneys

Using a semi-quantitative LC-MS/MS method, we detected several lipid classes and species in non-nephritic and nephritic kidneys. Figure 5A is the representative normal phase LC-MS chromatogram for six major classes of phospholipids found in the kidneys. The phosphotidylethanolamine (PE), PE(P-18:0/20:4), PE(P-18:1/20:4) and PE(P-18:0/20:4), which are the major storage depots for arachidonic acid were significantly increased in nephritic mice (Figure 5B–D). We also found a significant increase in the esterification of the sn-2 chain of PE with adrenic acid (C22:4) (P-18:0/22:4), the preferred substrate for lipid peroxidation[43] in the nephritic kidneys (Figure 5E). There was a differential distribution of lysophosphatidylethanolamines (LPE), phosphatidylethanolamines (PE), alkyl-phosphatidylethanolamine PE(O), and alkenyl-phosphatidylethanolamine PE(P) between non-nephritic and nephritic kidneys as depicted in the heat maps (Supplemental Figure 3A–D). These heat maps are represented as a means of pattern recognition, utilizing a color-code display of most differentially expressed species within in each class of lipids (Supplemental Figure 3E).

3.5 Kidney tubular injury and ferroptosis feature in lupus nephritis of different etiologies

Male (NZW X BXSB) F1 mice carry two copies of the *Tlr7* gene and develop proliferative nephritis by 16 weeks of age with clinical features of lupus (Supplemental Figure 4A) [44]. While not as severe as MRL/lpr females, the males presented renal pathology with glomerular and tubular injury. Increased gene expression of *Ngal* and *Kim1* (Supplemental Figure 4B–F) indicated damage to the proximal tubular cells with elevated oxidative stress (Supplemental Figure 4G–I). These mice also had reduced gene expression of both *Gclc* and *Gclm*, indicating an impaired glutathione synthesis pathway with concomitant decrease in the protein expression of GPX4 (Supplemental Figure 5A–D). In addition, we also observed an increased gene expression of *Acsl4* and *Aimf2* (Supplemental Figure 5E–F). These observations collectively identify tubular injury, impaired glutathione synthesis, and ferroptosis as a common denominator in models with different lupus nephritis etiology.

3.6 Impaired iron handling in kidney proximal tubular cells worsens tubular injury in the setting of primary glomerulonephritis

FtH1 levels were increased in nephritic mice (Figure 2E–F), but the functional importance of FtH1 in glomerulonephritis is unknown. Since iron deposits are not observed in the glomeruli of multiple glomerulopathies [13], including lupus nephritis (Figure 2), we choose to investigate role of FtH1 in the tubular segment of the kidney. Unlike the distal renal tubules, proximal tubular epithelial cells have a high abundance of FtH1 [13, 45]. Therefore, we induced nephrotoxic serum-induced glomerulonephritis[46] in transgenic mice deficient in *FtH1* expression only in the proximal tubules of the kidney ($FtH^{PT-/-}$). This tool permits us to tease out the fine molecular mechanisms of proximal tubular epithelial cell (PTEC) pathology following glomerular injury using mice lacking a particular gene selectively in their PTEC in settings of immune complex-mediated lupus-like nephritis. The genotype of the $FtH^{PT-/-}$ and $FtHPT^{+/+}$ littermate control mice is shown in Supplemental Figure 6A. Fourteen days following induction of glomerulonephritis, there was comparable proteinuria and glomerular immune complex deposits in $FtH^{PT-/-}$ and $FtHPT^{+/+}$ mice

(Supplemental Figure 6B–D). Similar to spontaneous lupus nephritis, the glomeruli were devoid of observable iron deposits (Supplemental Figure 6E–F). However, following the injection of nephrotoxic serum, dense but comparable Perl's detectable iron deposits were observed in both the $FtH^{PT-/-}$ and $FtH^{PT/+}$ mice (Supplemental Figure 6E–F, inset). As there was no injury in normal sheep serum (NSS) injected $FtHPT^{+/+}$ and $FtH^{PT-/-}$ and mice (Supplemental Figure 6B), iron deposits were not observed in the kidneys (data not shown). Hematoxylin-Eosin staining revealed extensive immune infiltrates in $FtHPT^{+/+}$ and $FtH^{PT-/-}$ mice (Figure 6A–B). However, compared to nephrotoxic serum injected $FtH^{PT+/+}$ littermate controls, $FtH^{PT-/-}$ mice had significantly more tubular epithelial cell necrosis (dark pink fragmented cytoplasm with no nuclei) with denudation of the basement membrane, tubular casts, dilatation, luminal debris (Figure 6A–B). To identify if ferroptosis was activated in this model, we probed the kidneys for ACSL4 and GPX4. While not expressed in NSS injected mice, ACSL4 was induced following the injection of nephrotoxic sheep serum (NTS) (Figure 6C) but was not significantly different between $FtHPT^{+/+}$ and $FtH^{PT-/-}$ mice, indicating onset of ferroptosis. However, compared NTS injected $FtHPT^{+/+}$ mice, $FtH^{PT-/-}$ mice had significantly lower GPX4 expression, suggesting exacerbated ferroptosis (Figure 6C–D). Increased gene expression of proximal tubular injury markers *Ngal* and *Kim1* in the nephrotoxic serum injected $FtH^{PT-/-}$ mice supported the histopathology and exacerbated ferroptosis (Figure 6 E–F). To further the importance of PTEC FtH1 in settings of increased iron and albumin (the two conditions observed in glomerulonephritis), we knocked down the FtH1 gene in human PTEC`s (HK-2 cells) (Figure 7A), without affecting the ferritin light chain (Figure 7B). Knocking down FtH1 in HK-2 cells or treating them with Fe^{2+} (ferrous sulfate) alone did not cause cell death as measured by LDH release (Figure 7C). Albumin treatment increased cell death comparably in scrambled siRNA and FtH1 knocked down cells (Figure 7C). However, albumin increased cell death in FtH1-knocked down cells treated with Fe^{2+} compared to KD cells treated with Fe^{2+} alone, as well as compared to control cells (Figure 7C). Since cell death was observed only after the addition of albumin with or without Fe, we looked for markers of ferroptosis in these two conditions. GPX4 expression was comparable and ACSL4 expression was not observed under basal conditions in FtH1 sufficient and knockdown cells (Figure 7D). GPX4 expression was comparably reduced following albumin and albumin + Fe treatment in FtH1 sufficient and FtH1 knockdown cells (Figure 7E). In comparison, ACSL4 expression was detected in FtH1 sufficient and knockdown cells only after the addition of albumin (Figure 7F and H), which was significantly elevated in the concomitant presence of Fe + albumin in FtH1 sufficient cells (Figure 7G and H). Loss of FtH1 further elevated the expression of this pro-ferroptotic molecule (Figure 7G and H). Collectively these data indicate that loss of FtH1 worsens ferroptosis and exacerbates proximal tubular epithelial cell injury in settings of glomerulonephritis.

3.7 Tubular ferroptosis is a prominent feature in human lupus nephritis and can be reversed *in vitro* by Liproxstatin-2, a new generation ferroptosis inhibitor

We next determined whether ferroptosis features in human lupus nephritis. Compared to non-nephritic controls, PAS-stained kidney biopsies of Class IV lupus nephritis patients showed regions of acute tubular injury with dilated tubules and casts (Supplemental Figure 7A). Compared to non lupus nephritis controls, we observed a higher expression

of 4HNE (lipid peroxidation, ferroptosis) in the tubular segments of human class IV lupus nephritis biopsies (Supplemental Figure 7B–D). This was similar to the 4HNE staining pattern observed in nephritic mice (Figure 4 C–D). Similarly, ACSL4 (a marker of ferroptosis) staining was primarily observed in the tubular segments of the kidney biopsies (Supplemental Figure 7E–G). These data indicate the occurrence of ferroptosis in the kidney tubules of human Class IV lupus nephritis. Since ferroptosis was primarily observed in the tubular segments and IgG, anti-dsDNA antibodies, and excess protein activate ROS-sensitive pathways that lead to tubular-injury [9] we evaluated the effect of Class IV lupus nephritis patient's serum on HK-2 cells. We choose this population as it involves diffuse lupus nephritis involving 50% or more of glomeruli, which indicates severe LN requiring more-intensive therapy. Though the iron content of healthy controls and Class IV lupus nephritis patients' serum was comparable (Figure 8A), only patients' serum rapidly and significantly increased the expression of transferrin receptor 1 (TfR1), the major iron import protein (Figure 8B–C). Furthermore, only patients' serum attenuated the expression of SLC7A11 precursor mRNA and mRNA suggesting transcriptional inhibition (Figure 8D–E). The patients' serum also significantly increased markers of oxidative stress (Figure 9A–B), ferroptosis (Figure 9C–E), inflammation and injury in HK-2 cells (Figure 9F–G). All these pathological features were significantly mitigated by Liproxstatin-2 (Figure9A–D). Importantly, Liproxstatin-2 demonstrated therapeutic benefit when administered an hour after the addition of lupus nephritis serum (Figure9A–G). Administering Liproxstatin-2, 4h after serum addition had no beneficial effect (Figure9A–G).

4. Discussion

The present study highlights renal tubular ferroptosis as a pathological feature in both human and murine lupus nephritis, thus identifying a novel druggable target to treat a disease still managed mainly by immunosuppression. Additionally, we highlight the importance of iron sequestration and tubular ferroptosis and injury in primary glomerulonephritis and demonstrate. Furthermore, lupus nephritis serum components activate the iron uptake program and inhibit transcription of cystine uptake protein to potentially sensitize human PTEC to ferroptosis which can be reversed by a new generation ferroptosis inhibitor, Liproxstatin-2. These are new findings in the field. In this study we compared non nephritic and nephritic MRL/lpr mice instead of age matched MRL/Mpj mice which have the same genetic background without FAS-deficiency as they exhibit mild autoimmune manifestations including renal immune complex deposits and Sjogren syndrome [47–49] which can perturb their iron metabolism.

ACSL4, a key ferroptosis executioner and dictates ferroptosis sensitivity by shaping cellular lipid composition [43]. The PÈs can be hydrolyzed to liberate arachidonic acid [50, 51]. ACSL4 ligates arachidonic acid with CoA to generate arachidonoyl-CoA, which is conjugated to PE to generate esterified-PE[19]. We found a significant increase in esterified sn-2 chain of PE (P-18:0/22:4). These esterified PE conjugates are oxidized by lipoxygenases to generate toxic lipid hydroperoxides, the proximate executors of ferroptosis [43, 52]. Cells utilize SLC7A11 mediated cystine import and GPX4 as a defense mechanism to counter ferroptosis [53]. Cystine availability is the rate-limiting step in the biosynthesis of glutathione (GSH)[40] which is a cofactor of GPX4[54, 55]. Nephritic kidneys have

attenuated expression of SLC7A11, as well as *Gclc* and *Gclm*, the gene products that make up the enzyme GCL indicating impaired GCL activity. Reduced GCL activity directly inhibits GSH synthesis [56] and may account for the observed reduction in GPX4 in nephritic kidneys which is critical to reduce toxic lipid peroxides to nontoxic lipid alcohols and prevent ferroptosis[22, 57–59]. This is summarized in figure 10.

We have previously published that compounds that induce FtH1 protect against lupus nephritis [17]. While FtH1 deficiency in proximal kidney tubules worsens acute kidney injury and fibrosis [27, 28], its influence on the outcomes of tubular injury following immune complex glomerulonephritis is unexplored. Here we found that mice with FtH1 deficient PTEC were more susceptible to injury following induction of glomerulonephritis. This was notably independent of the extent of glomerular injury and was associated with an increase in ACSL4 and an attenuation of GPX4 expression, again a new finding in the field. While iron deficiency does not affect the development of glomerular disease in nephrotoxic serum nephritis, it mitigates tubulo-interstitial disease and renal functional deterioration [15]. Our study furthers these observations by directly identifying ferroptosis as a contributing factor in lupus nephritis and lend support to the observations that the extent of tubular injury is independent of glomerular pathology in human glomerulonephritis [5, 60]. We speculate that the ability of FtH1-deficient proximal tubular cells to handle iron in absence of injurious agent may be attributable to light chain ferritin (FtL) [13, 61, 62].

Of clinical relevance we demonstrate that human lupus nephritis patients' serum induced an iron import program (increased expression of TfR1) and transcriptionally inhibited SLC7A11 (attenuated precursor mRNA of SLC7A11), both of which can render PTEC susceptible to ferroptosis. Unlike our *in vivo* observations where GPX4 protein expression levels were attenuated in nephritic mice, class IV lupus nephritis serum induced the gene expression of *GPX4* in healthy PTECs. This discrepancy could be due to the difference in the chronicity of the kidney disease versus the acute nature of the *in vitro* studies. Healthy PTEC may upregulate *GPX4* as a protective response to the different serum components. While our study does not distinguish whether autoantibodies of different specificities or cytokine milieu are needed for proximal tubular epithelial cells ferroptosis, the prophylactic and therapeutic benefit of Liproxstain-2, provides a novel alternative to mitigate proximal tubular epithelial cells pathology even in severe lupus nephritis (class IV).

5. Conclusion

The concept that chronic inflammatory state significantly downregulates GSH metabolism genes in proximal tubules, making the cells vulnerable to ferroptosis and worsens the outcomes of kidney disease is now documented[63–67]. While apoptosis, NETosis, necroptosis, pyroptosis, and autophagy play a role in tissue damage and immune dysregulation in lupus nephritis[68], our study for the first time identifies a novel druggable mechanism contributing to tubular pathology during the evolution of lupus nephritis, laying the groundwork for future investigations of ferroptosis inhibitors in lupus nephritis.

Supplementary Material

Refer to Web version on PubMed Central for supplementary material.

Acknowledgments

The authors are thankful to Dr. Volker Haase (Vanderbilt University) for providing the PepckCre mice.

Funding

These studies were supported by grants from Vifor Pharma (P0213104, P0226952) to YS, NIH (R01AI135128) to BM, NIH (R01AI128901) to Laurence Morel and in part by a NIH Shared Instrumentation Grant (1S10OD018141–01A1) to NDD.

References

[1]. Schwartz N, Goilav B, Putterman C, The pathogenesis, diagnosis and treatment of lupus nephritis, Curr Opin Rheumatol, 26 (2014) 502–509. [PubMed: 25014039]

[2]. Frangou E, Georgakis S, Bertsias G, Update on the cellular and molecular aspects of lupus nephritis, Clin Immunol, 216 (2020) 108445. [PubMed: 32344016]

[3]. Song K, Liu L, Zhang X, Chen X, An update on genetic susceptibility in lupus nephritis, Clin Immunol, 215 (2020) 108389. [PubMed: 32245575]

[4]. Dooley MA, Jayne D, Ginzler EM, Isenberg D, Olsen NJ, Wofsy D, Eitner F, Appel GB, Contreras G, Lisk L, Solomons N, Group A, Mycophenolate versus azathioprine as maintenance therapy for lupus nephritis, N Engl J Med, 365 (2011) 1886–1895. [PubMed: 22087680]

[5]. Rijnink EC, Teng YKO, Wilhelmus S, Almekinders M, Wolterbeek R, Cransberg K, Bruijn JA, Bajema IM, Clinical and Histopathologic Characteristics Associated with Renal Outcomes in Lupus Nephritis, Clinical journal of the American Society of Nephrology : CJASN, 12 (2017) 734–743. [PubMed: 28473317]

[6]. Hong S, Healy H, Kassianos AJ, The Emerging Role of Renal Tubular Epithelial Cells in the Immunological Pathophysiology of Lupus Nephritis, Frontiers in immunology, 11 (2020) 578952. [PubMed: 33072122]

[7]. Wilson PC, Kashgarian M, Moeckel G, Interstitial inflammation and interstitial fibrosis and tubular atrophy predict renal survival in lupus nephritis, Clin Kidney J, 11 (2018) 207–218. [PubMed: 29644061]

[8]. Davidson A, What is damaging the kidney in lupus nephritis?, Nat Rev Rheumatol, 12 (2016) 143–153. [PubMed: 26581344]

[9]. Yung S, Ng CY, Au KY, Cheung KF, Zhang Q, Zhang C, Yap DY, Chau MK, Chan TM, Binding of anti-dsDNA antibodies to proximal tubular epithelial cells contributes to renal tubulointerstitial inflammation, Clin Sci (Lond), 131 (2017) 49–67. [PubMed: 27780843]

[10]. Yung S, Chan TM, Anti-dsDNA antibodies and resident renal cells - Their putative roles in pathogenesis of renal lesions in lupus nephritis, Clin Immunol, 185 (2017) 40–50. [PubMed: 27612436]

[11]. Perl A, Oxidative stress in the pathology and treatment of systemic lupus erythematosus, Nat Rev Rheumatol, 9 (2013) 674–686. [PubMed: 24100461]

[12]. Shao X, Yang R, Yan M, Li Y, Du Y, Raman I, Zhang B, Wakeland EK, Igarashi P, Mohan C, Li QZ, Inducible expression of kallikrein in renal tubular cells protects mice against spontaneous lupus nephritis, Arthritis Rheum, 65 (2013) 780–791. [PubMed: 23280471]

[13]. van Raaij S, van Swelm R, Bouman K, Cliteur M, van den Heuvel MC, Pertijs J, Patel D, Bass P, van Goor H, Unwin R, Srai SK, Swinkels D, Tubular iron deposition and iron handling proteins in human healthy kidney and chronic kidney disease, Sci Rep, 8 (2018) 9353. [PubMed: 29921869]

[14]. Marks ES, Bonnemaison ML, Brusnahan SK, Zhang W, Fan W, Garrison JC, Boesen EI, Renal iron accumulation occurs in lupus nephritis and iron chelation delays the onset of albuminuria, Sci Rep, 7 (2017) 12821. [PubMed: 28993663]

[15]. Alfrey AC, Froment DH, Hammond WS, Role of iron in the tubulo-interstitial injury in nephrotoxic serum nephritis, Kidney international, 36 (1989) 753–759. [PubMed: 2615188]

[16]. Winterbourn CC, Toxicity of iron and hydrogen peroxide: the Fenton reaction, Toxicol Lett, 82-83 (1995) 969–974.

[17]. Scindia Y, Wlazlo E, Ghias E, Cechova S, Loi V, Leeds J, Ledesma J, Helen C, Swaminathan S, Modulation of iron homeostasis with hepcidin ameliorates spontaneous murine lupus nephritis, Kidney international, 98 (2020) 100–115. [PubMed: 32444136]

[18]. Zhao M, Li MY, Gao XF, Jia SJ, Gao KQ, Zhou Y, Zhang HH, Huang Y, Wang J, Wu HJ, Lu QJ, Downregulation of BDH2 modulates iron homeostasis and promotes DNA demethylation in CD4(+) T cells of systemic lupus erythematosus, Clin Immunol, 187 (2018) 113–121. [PubMed: 29113828]

[19]. Kagan VE, Mao G, Qu F, Angeli JP, Doll S, Croix CS, Dar HH, Liu B, Tyurin VA, Ritov VB, Kapralov AA, Amoscato AA, Jiang J, Anthonymuthu T, Mohammadyani D, Yang Q, Proneth B, Klein-Seetharaman J, Watkins S, Bahar I, Greenberger J, Mallampalli RK, Stockwell BR, Tyurina YY, Conrad M, Bayir H, Oxidized arachidonic and adrenic PEs navigate cells to ferroptosis, Nat Chem Biol, 13 (2017) 81–90. [PubMed: 27842066]

[20]. Jiang X, Stockwell BR, Conrad M, Ferroptosis: mechanisms, biology and role in disease, Nat Rev Mol Cell Biol, 22 (2021) 266–282. [PubMed: 33495651]

[21]. Dixon SJ, Lemberg KM, Lamprecht MR, Skouta R, Zaitsev EM, Gleason CE, Patel DN, Bauer AJ, Cantley AM, Yang WS, Morrison B 3rd, Stockwell BR, Ferroptosis: an iron-dependent form of nonapoptotic cell death, Cell, 149 (2012) 1060–1072. [PubMed: 22632970]

[22]. Friedmann Angeli JP, Schneider M, Proneth B, Tyurina YY, Tyurin VA, Hammond VJ, Herbach N, Aichler M, Walch A, Eggenhofer E, Basavarajappa D, Radmark O, Kobayashi S, Seibt T, Beck H, Neff F, Esposito I, Wanke R, Forster H, Yefremova O, Heinrichmeyer M, Bornkamm GW, Geissler EK, Thomas SB, Stockwell BR, O'Donnell VB, Kagan VE, Schick JA, Conrad M, Inactivation of the ferroptosis regulator Gpx4 triggers acute renal failure in mice, Nat Cell Biol, 16 (2014) 1180–1191. [PubMed: 25402683]

[23]. Belavgeni A, Meyer C, Stumpf J, Hugo C, Linkermann A, Ferroptosis and Necroptosis in the Kidney, Cell Chem Biol, 27 (2020) 448–462. [PubMed: 32302582]

[24]. Frostegard J, Svenungsson E, Wu R, Gunnarsson I, Lundberg IE, Klareskog L, Horkko S, Witztum JL, Lipid peroxidation is enhanced in patients with systemic lupus erythematosus and is associated with arterial and renal disease manifestations, Arthritis Rheum, 52 (2005) 192–200. [PubMed: 15641060]

[25]. Li P, Jiang M, Li K, Li H, Zhou Y, Xiao X, Xu Y, Krishfield S, Lipsky PE, Tsokos GC, Zhang X, Glutathione peroxidase 4-regulated neutrophil ferroptosis induces systemic autoimmunity, Nat Immunol, 22 (2021) 1107–1117. [PubMed: 34385713]

[26]. Wang W, Lin Z, Feng J, Liang Q, Zhao J, Zhang G, Chen R, Fu R, Identification of ferroptosis-related molecular markers in glomeruli and tubulointerstitium of lupus nephritis, Lupus, (2022) 9612033221102076.

[27]. Bolisetty S, Zarjou A, Hull TD, Traylor AM, Perianayagam A, Joseph R, Kamal AI, Arosio P, Soares MP, Jeney V, Balla J, George JF, Agarwal A, Macrophage and epithelial cell H-ferritin expression regulates renal inflammation, Kidney international, 88 (2015) 95–108. [PubMed: 25874599]

[28]. Zarjou A, Bolisetty S, Joseph R, Traylor A, Apostolov EO, Arosio P, Balla J, Verlander J, Darshan D, Kuhn LC, Agarwal A, Proximal tubule H-ferritin mediates iron trafficking in acute kidney injury, The Journal of clinical investigation, 123 (2013) 4423–4434. [PubMed: 24018561]

[29]. Kaneko Y, Nimmerjahn F, Madaio MP, Ravetch JV, Pathology and protection in nephrotoxic nephritis is determined by selective engagement of specific Fc receptors, J Exp Med, 203 (2006) 789–797. [PubMed: 16520389]

[30]. Mohan C, Alas E, Morel L, Yang P, Wakeland EK, Genetic dissection of SLE pathogenesis. Sle1 on murine chromosome 1 leads to a selective loss of tolerance to H2A/H2B/DNA subnucleosomes, The Journal of clinical investigation, 101 (1998) 1362–1372.

[31]. Bligh EG, Dyer WJ, A rapid method of total lipid extraction and purification, Can J Biochem Physiol, 37 (1959) 911–917. [PubMed: 13671378]

[32]. van Raaij SEG, Srai SKS, Swinkels DW, van Swelm RPL, Iron uptake by ZIP8 and ZIP14 in human proximal tubular epithelial cells, Biometals, 32 (2019) 211–226. [PubMed: 30806852]

[33]. Cozzi A, Corsi B, Levi S, Santambrogio P, Albertini A, Arosio P, Overexpression of wild type and mutated human ferritin H-chain in HeLa cells: in vivo role of ferritin ferroxidase activity, The Journal of biological chemistry, 275 (2000) 25122–25129. [PubMed: 10833524]

[34]. Wlazlo E, Mehrad B, Morel L, Scindia Y, Iron Metabolism: An Under Investigated Driver of Renal Pathology in Lupus Nephritis, Front Med (Lausanne), 8 (2021) 643686. [PubMed: 33912577]

[35]. Torti FM, Torti SV, Regulation of ferritin genes and protein, Blood, 99 (2002) 3505–3516. [PubMed: 11986201]

[36]. Reilly CM, Farrelly LW, Viti D, Redmond ST, Hutchison F, Ruiz P, Manning P, Connor J, Gilkeson GS, Modulation of renal disease in MRL/lpr mice by pharmacologic inhibition of inducible nitric oxide synthase, Kidney international, 61 (2002) 839–846. [PubMed: 11849435]

[37]. Linkermann A, Skouta R, Himmerkus N, Mulay SR, Dewitz C, De Zen F, Prokai A, Zuchtriegel G, Krombach F, Welz PS, Weinlich R, Vanden Berghe T, Vandenabeele P, Pasparakis M, Bleich M, Weinberg JM, Reichel CA, Brasen JH, Kunzendorf U, Anders HJ, Stockwell BR, Green DR, Krautwald S, Synchronized renal tubular cell death involves ferroptosis, Proceedings of the National Academy of Sciences of the United States of America, 111 (2014) 16836–16841. [PubMed: 25385600]

[38]. Deng F, Sharma I, Dai Y, Yang M, Kanwar YS, Myo-inositol oxygenase expression profile modulates pathogenic ferroptosis in the renal proximal tubule, The Journal of clinical investigation, 129 (2019) 5033–5049. [PubMed: 31437128]

[39]. Nakamura E, Sato M, Yang H, Miyagawa F, Harasaki M, Tomita K, Matsuoka S, Noma A, Iwai K, Minato N, 4F2 (CD98) heavy chain is associated covalently with an amino acid transporter and controls intracellular trafficking and membrane topology of 4F2 heterodimer, The Journal of biological chemistry, 274 (1999) 3009–3016. [PubMed: 9915839]

[40]. Stockwell BR, Friedmann Angeli JP, Bayir H, Bush AI, Conrad M, Dixon SJ, Fulda S, Gascon S, Hatzios SK, Kagan VE, Noel K, Jiang X, Linkermann A, Murphy ME, Overholtzer M, Oyagi A, Pagnussat GC, Park J, Ran Q, Rosenfeld CS, Salnikow K, Tang D, Torti FM, Torti SV, Toyokuni S, Woerpel KA, Zhang DD, Ferroptosis: A Regulated Cell Death Nexus Linking Metabolism, Redox Biology, and Disease, Cell, 171 (2017) 273–285. [PubMed: 28985560]

[41]. Chen Y, Shertzer HG, Schneider SN, Nebert DW, Dalton TP, Glutamate cysteine ligase catalysis: dependence on ATP and modifier subunit for regulation of tissue glutathione levels, The Journal of biological chemistry, 280 (2005) 33766–33774. [PubMed: 16081425]

[42]. Forcina GC, Dixon SJ, GPX4 at the Crossroads of Lipid Homeostasis and Ferroptosis, Proteomics, 19 (2019) e1800311. [PubMed: 30888116]

[43]. Doll S, Proneth B, Tyurina YY, Panzilius E, Kobayashi S, Ingold I, Irmler M, Beckers J, Aichler M, Walch A, Prokisch H, Trumbach D, Mao G, Qu F, Bayir H, Fullekrug J, Scheel CH, Wurst W, Schick JA, Kagan VE, Angeli JP, Conrad M, ACSL4 dictates ferroptosis sensitivity by shaping cellular lipid composition, Nat Chem Biol, 13 (2017) 91–98. [PubMed: 27842070]

[44]. Baccala R, Gonzalez-Quintial R, Schreiber RD, Lawson BR, Kono DH, Theofilopoulos AN, Anti-IFN-alpha/beta receptor antibody treatment ameliorates disease in lupus-predisposed mice, Journal of immunology, 189 (2012) 5976–5984.

[45]. Zhang D, Meyron-Holtz E, Rouault TA, Renal iron metabolism: transferrin iron delivery and the role of iron regulatory proteins, Journal of the American Society of Nephrology : JASN, 18 (2007) 401–406. [PubMed: 17229905]

[46]. Fu Y, Du Y, Mohan C, Experimental anti-GBM disease as a tool for studying spontaneous lupus nephritis, Clin Immunol, 124 (2007) 109–118. [PubMed: 17640604]

[47]. Jabs DA, Prendergast RA, Rorer EM, Hudson AP, Whittum-Hudson JA, Cytokines in autoimmune lacrimal gland disease in MRL/MpJ mice, Invest Ophthalmol Vis Sci, 42 (2001) 2567–2571. [PubMed: 11581200]

[48]. Jabs DA, Prendergast RA, Campbell AL, Lee B, Akpek EK, Gerard HC, Hudson AP, Whittum-Hudson JA, Autoimmune Th2-mediated dacryoadenitis in MRL/MpJ mice becomes

Th1-mediated in IL-4 deficient MRL/MpJ mice, Invest Ophthalmol Vis Sci, 48 (2007) 5624–5629. [PubMed: 18055812]

[49]. McGaha TL, Karlsson MC, Ravetch JV, FcgammaRIIB deficiency leads to autoimmunity and a defective response to apoptosis in Mrl-MpJ mice, Journal of immunology, 180 (2008) 5670–5679.

[50]. Ford DA, Gross RW, Plasmenylethanolamine is the major storage depot for arachidonic acid in rabbit vascular smooth muscle and is rapidly hydrolyzed after angiotensin II stimulation, Proceedings of the National Academy of Sciences of the United States of America, 86 (1989) 3479–3483. [PubMed: 2498871]

[51]. Tomita-Yamaguchi M, Babich JF, Baker RC, Santoro TJ, Incorporation, distribution, and turnover of arachidonic acid within membrane phospholipids of B220+ T cells from autoimmune-prone MRL-lpr/lpr mice, J Exp Med, 171 (1990) 787–800. [PubMed: 2106567]

[52]. Kuwata H, Hara S, Role of acyl-CoA synthetase ACSL4 in arachidonic acid metabolism, Prostaglandins Other Lipid Mediat, 144 (2019) 106363. [PubMed: 31306767]

[53]. Ye Y, Chen A, Li L, Liang Q, Wang S, Dong Q, Fu M, Lan Z, Li Y, Liu X, Ou JS, Lu L, Yan J, Repression of the antiporter SLC7A11/glutathione/glutathione peroxidase 4 axis drives ferroptosis of vascular smooth muscle cells to facilitate vascular calcification, Kidney international, (2022).

[54]. Brigelius-Flohe R, Maiorino M, Glutathione peroxidases, Biochimica et biophysica acta, 1830 (2013) 3289–3303. [PubMed: 23201771]

[55]. Yang WS, SriRamaratnam R, Welsch ME, Shimada K, Skouta R, Viswanathan VS, Cheah JH, Clemons PA, Shamji AF, Clish CB, Brown LM, Girotti AW, Cornish VW, Schreiber SL, Stockwell BR, Regulation of ferroptotic cancer cell death by GPX4, Cell, 156 (2014) 317–331. [PubMed: 24439385]

[56]. Lu SC, Regulation of glutathione synthesis, Molecular aspects of medicine, 30 (2009) 42–59. [PubMed: 18601945]

[57]. Hagberg JP, [Can a therapy be neutral? Value neutrality and some different views on man in the therapy community], Tidsskr Nor Laegeforen, 94 (1974) 2295–2299. [PubMed: 4439385]

[58]. Yang WS, Stockwell BR, Synthetic lethal screening identifies compounds activating iron-dependent, nonapoptotic cell death in oncogenic-RAS-harboring cancer cells, Chem Biol, 15 (2008) 234–245. [PubMed: 18355723]

[59]. Chen L, Na R, Danae McLane K, Thompson CS, Gao J, Wang X, Ran Q, Overexpression of ferroptosis defense enzyme Gpx4 retards motor neuron disease of SOD1G93A mice, Sci Rep, 11 (2021) 12890. [PubMed: 34145375]

[60]. Hsieh C, Chang A, Brandt D, Guttikonda R, Utset TO, Clark MR, Predicting outcomes of lupus nephritis with tubulointerstitial inflammation and scarring, Arthritis Care Res (Hoboken), 63 (2011) 865–874. [PubMed: 21309006]

[61]. Zarjou A, Black LM, McCullough KR, Hull TD, Esman SK, Boddu R, Varambally S, Chandrashekar DS, Feng W, Arosio P, Poli M, Balla J, Bolisetty S, Ferritin Light Chain Confers Protection Against Sepsis-Induced Inflammation and Organ Injury, Frontiers in immunology, 10 (2019) 131. [PubMed: 30804939]

[62]. Fan Y, Zhang J, Cai L, Wang S, Liu C, Zhang Y, You L, Fu Y, Shi Z, Yin Z, Luo L, Chang Y, Duan X, The effect of anti-inflammatory properties of ferritin light chain on lipopolysaccharide-induced inflammatory response in murine macrophages, Biochimica et biophysica acta, 1843 (2014) 2775–2783. [PubMed: 24983770]

[63]. Ide S, Kobayashi Y, Ide K, Strausser SA, Abe K, Herbek S, O'Brien LL, Crowley SD, Barisoni L, Tata A, Tata PR, Souma T, Ferroptotic stress promotes the accumulation of pro-inflammatory proximal tubular cells in maladaptive renal repair, Elife, 10 (2021).

[64]. Li S, Zheng L, Zhang J, Liu X, Wu Z, Inhibition of ferroptosis by up-regulating Nrf2 delayed the progression of diabetic nephropathy, Free radical biology & medicine, 162 (2021) 435–449. [PubMed: 33152439]

[65]. Zhang B, Chen X, Ru F, Gan Y, Li B, Xia W, Dai G, He Y, Chen Z, Liproxstatin-1 attenuates unilateral ureteral obstruction-induced renal fibrosis by inhibiting renal tubular epithelial cells ferroptosis, Cell Death Dis, 12 (2021) 843. [PubMed: 34511597]

[66]. Wang Y, Bi R, Quan F, Cao Q, Lin Y, Yue C, Cui X, Yang H, Gao X, Zhang D, Ferroptosis involves in renal tubular cell death in diabetic nephropathy, Eur J Pharmacol, 888 (2020) 173574. [PubMed: 32976829]

[67]. Kim S, Kang SW, Joo J, Han SH, Shin H, Nam BY, Park J, Yoo TH, Kim G, Lee P, Park JT, Characterization of ferroptosis in kidney tubular cell death under diabetic conditions, Cell Death Dis, 12 (2021) 160. [PubMed: 33558472]

[68]. Mistry P, Kaplan MJ, Cell death in the pathogenesis of systemic lupus erythematosus and lupus nephritis, Clin Immunol, 185 (2017) 59–73. [PubMed: 27519955]

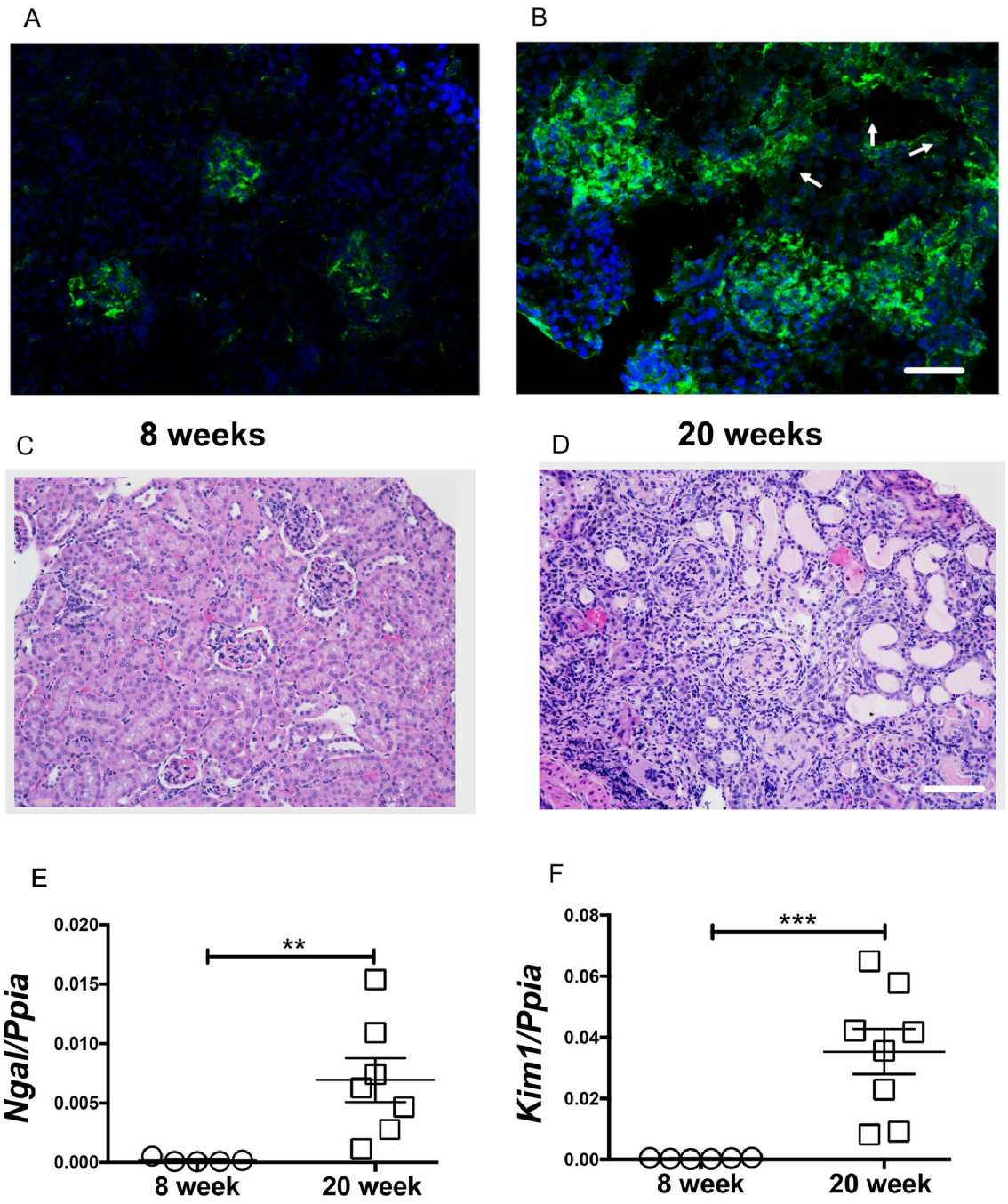

Figure 1. Tubular injury is a distinct feature in lupus nephritis.

Glomerular immune complexes were observed in 8-week-old non nephritic female MRL/lpr mice (A). At 20-weeks of age, glomerular and tubular immune complex deposits are evident (arrow points to the tubules) (B). Compared to 8-week-old female (C), the renal histology (H&E) at 20 weeks showed severe periglomerular and interstitial immune infiltrates. Along with the traditional glomerular injury, large number of a-nuclear tubules, tubular cast are also evident (D). Scale bar = 50 μm and 100 μm. The tubular injury marker *Ngal* and *Kim1* were significantly elevated in 20-week-old nephritic mice (E-F). Statistical significance was

determined by 2-tailed Mann-Whitney test and represented as mean ± SEM. **P < 0.01, ***P < 0.001.

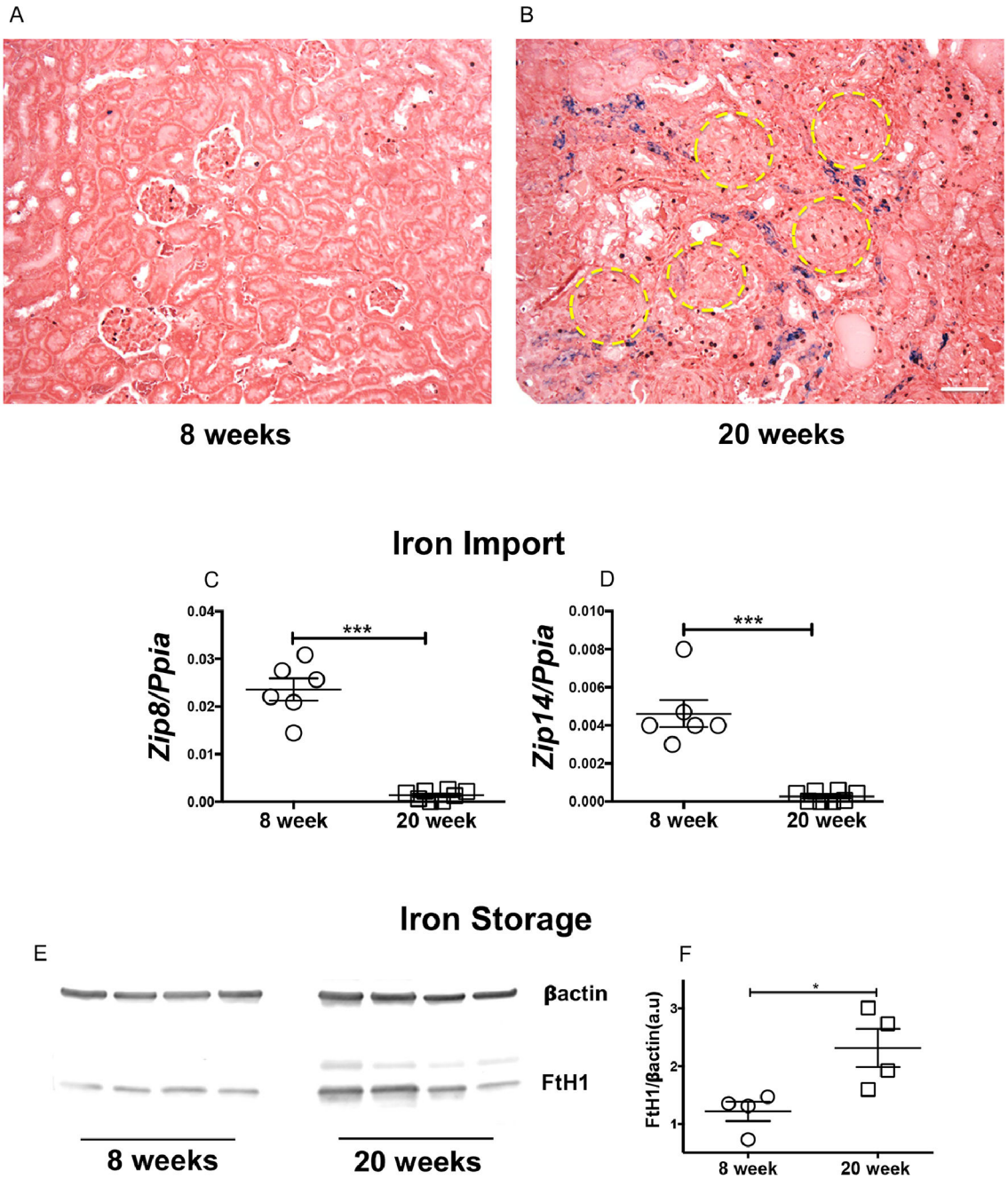

Figure 2. Iron accumulates in the renal tubular segments of nephritic mice and associated with attenuation in iron import program and elevation in iron storage machinery.

Formalin fixed kidney sections from 8- and 20-week-old female MRL/lpr mice were stained for Perl`s detectable iron, most of which was detected in the interstitium and tubular segments of nephritic mice (A-B). Scale bar = 50 μm. Though severely injured, the glomeruli (yellow circles) were devoid of iron deposits (B). Renal gene signature of iron importers, *Zip8* and *Zip14* was reduced in 20-week-old nephritic female MRL/lpr mice (C-D). Increase in renal iron was associated with an elevated expression of heavy chain ferritin (FtH), the endogenous iron sequestration protein (E-F). Statistical significance was

determined by 2-tailed Mann-Whitney test and plotted as mean ± SEM. *P < 0.01, ***P < 0.0001.

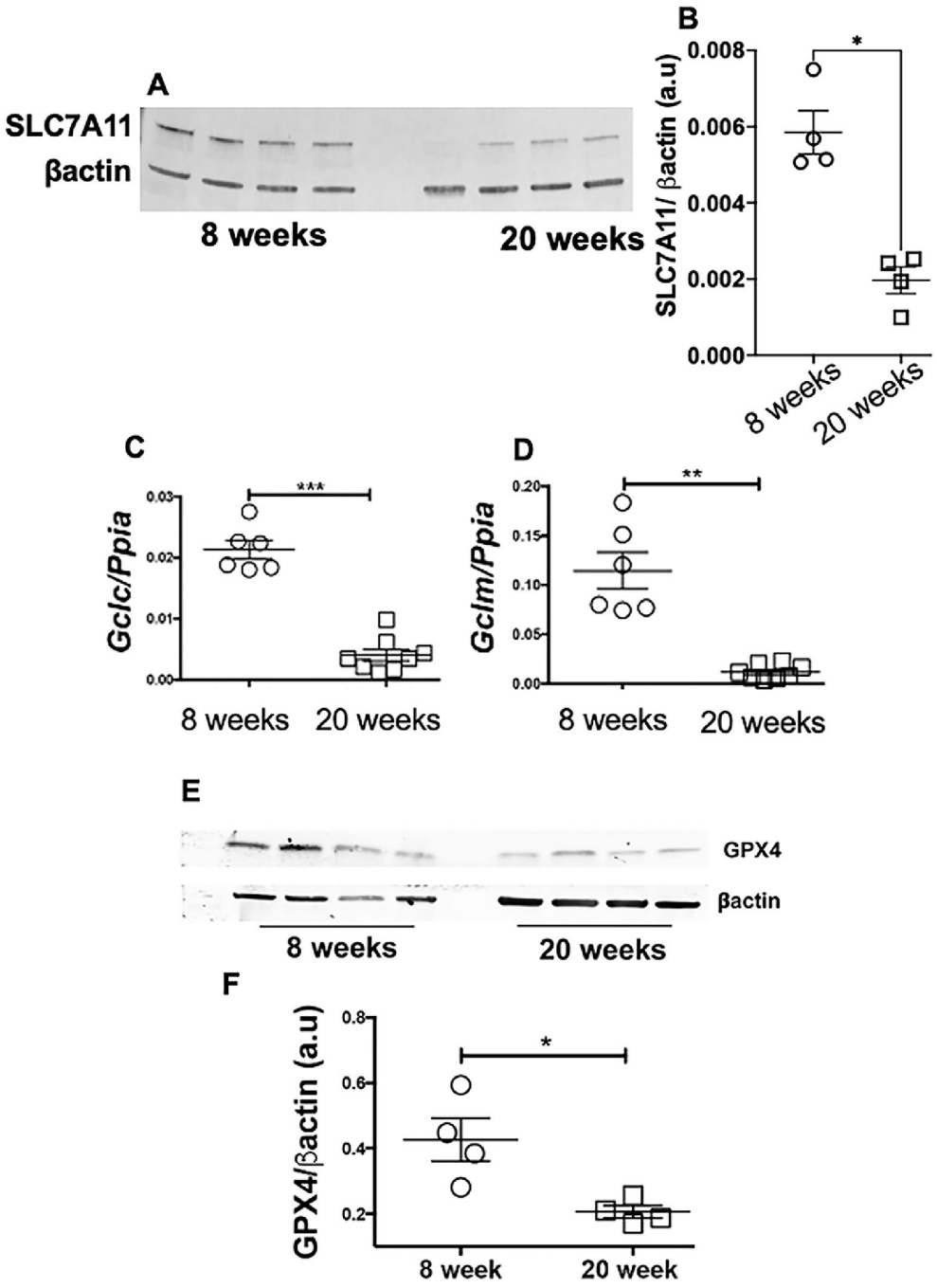

Figure 3. Lupus nephritis is associated with attenuated expression of cystine importer, impairments in glutathione biosynthesis pathway and low GPX4 expression.

Nephritic female MRL/lpr mice had a attenuated expression of SLC7A11, the cystine-glutamate antiporter and a highly specific cystine importer (A-B), lower expression of *Gclc* (C) and *Gclm* (D), gene products that constitute glutamate cysteine ligase (GCL), the activity of which determines de novo glutathione synthesis. Compared to 8-week-old MRL/lpr females, 20-week-old nephritic females had significantly lower expression of GPX4, the glutathione dependent ferroptosis inhibitor (E-F).

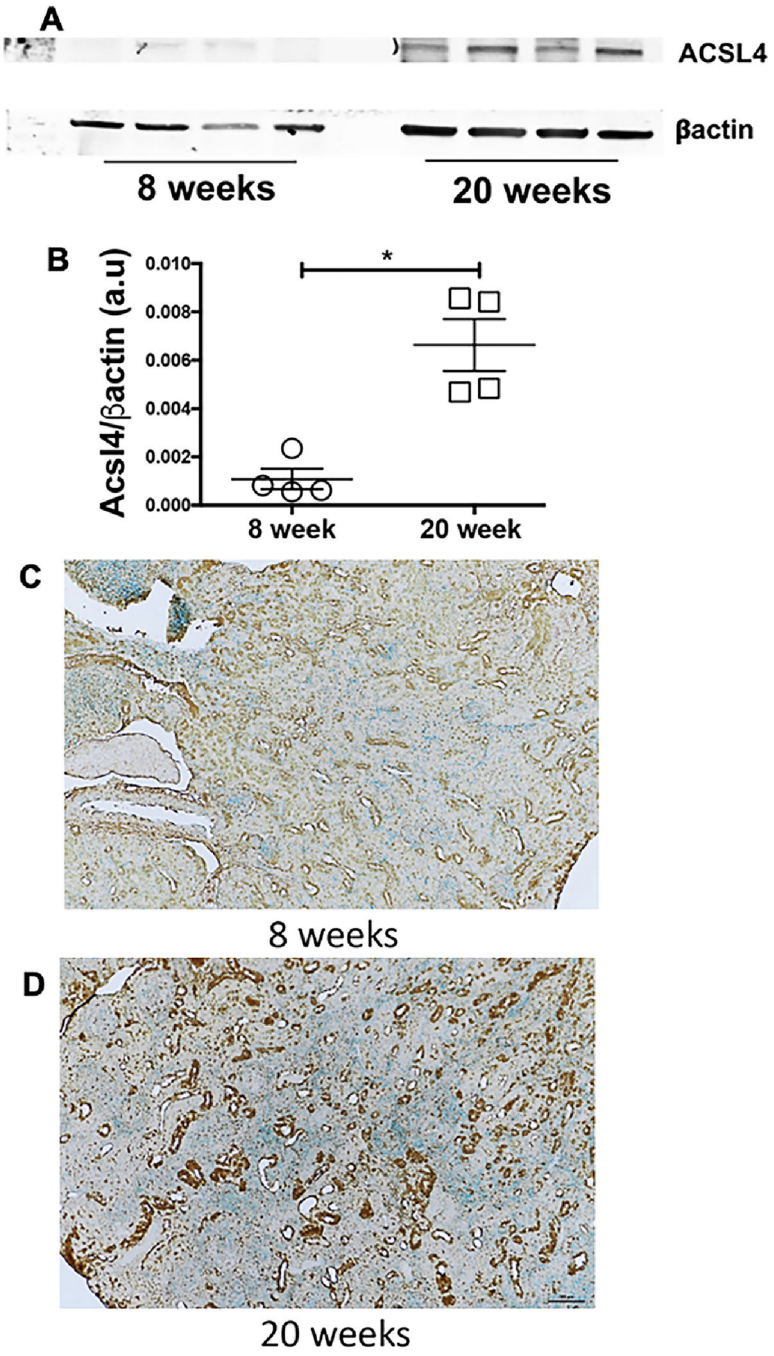

Figure 4. Increased expression of pro-ferroptosis enzyme ACSL4 and tubular lipid peroxidation in the kidneys of nephritic mice.

The expression of ACSL4, the enzymes that dictates the shape of lipid the ferroptosis executioner was significantly elevated (A-B). Compared to non-nephritic 8-week-old MRL/lpr females (C), the nephritic kidneys of MRL/lpr females stain more intensely for 4-HNE, a lipid peroxidation marker (D). Most of the staining is in the tubular segments, the area of iron accumulation. Scale bar = 50 μm. Statistical significance was determined by 2-tailed Mann-Whitney test. Data are plotted as mean ± SEM. *P < 0.05.

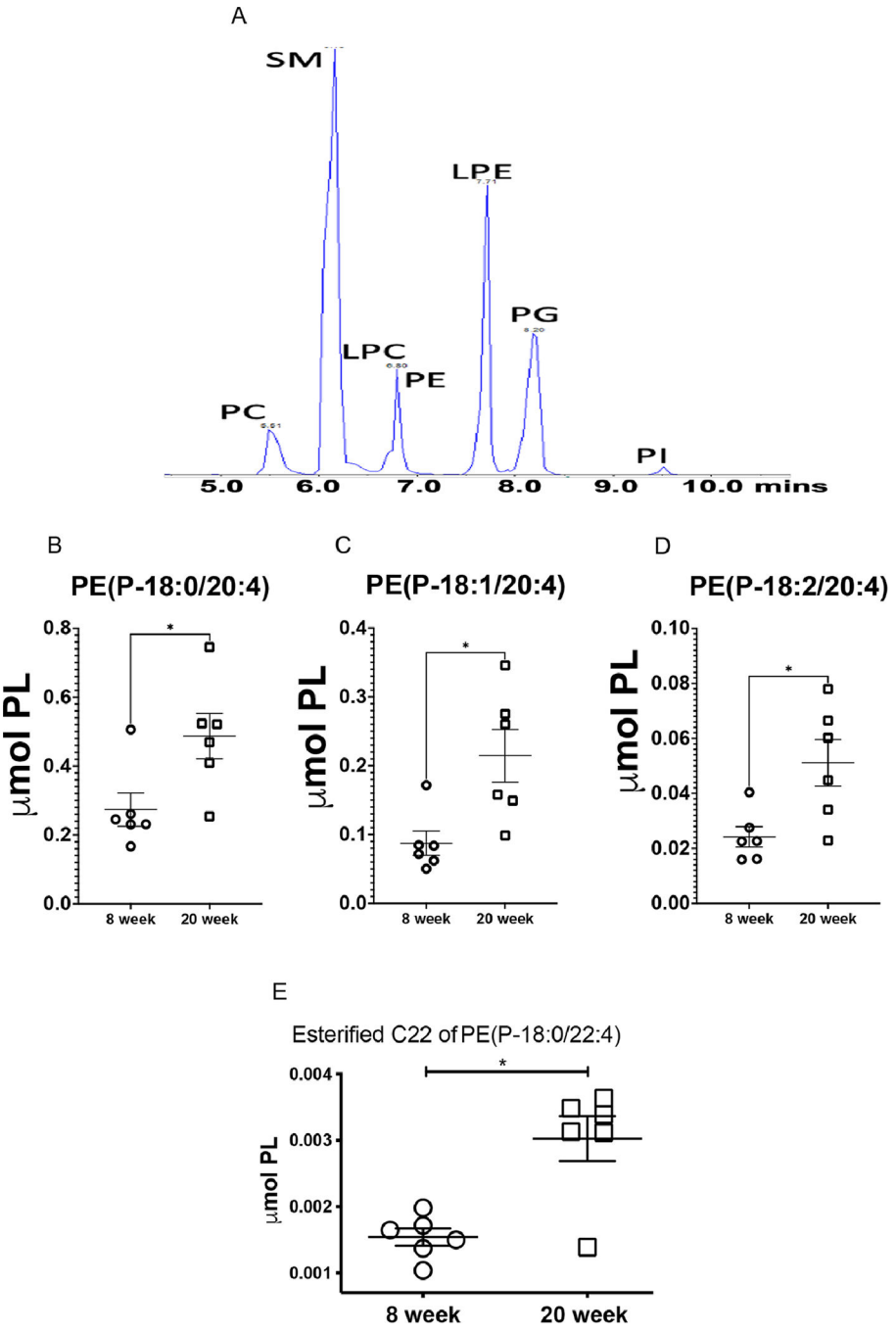

Figure 5. Differential renal lipid profile and increased esterification of phosphatidylethanolamine (PE) SN1 chain in nephritic mice.

8-week-old (non-nephritic) and 20-week-old (nephritic) MRL/lpr female kidneys were analyzed by semi-targeted LS-MS for their lipid profile and content. Representative normal phase LC-MS/MS chromatogram for six major classes of phospholipids: phosphatidylcholine (PC), sphingomyelin (SM),lysophophatidylcholine(PLC),phosphotidylethanolamine(PE),lysophosphotidylethanol amin e (LPE), phosphotidylglycerol (PG), and phosphotidylinostitol (PI) (A). Nephritic mice (20-week-old) had significantly higher concentrations of PE(P-18:0/20:4) (B),

PE(P-18:1/20:4) (C) and PE(P-18:0/20:4) (D), the major storage depots for arachidonic acid. Nephritis was also associated with an increase in esterified C22 chain of PE (P-18:0/22:4), the preferred substrate for ferroptosis (E). (n = 6 each). Statistical significance was determined by 2-tailed Mann-Whitney test. Data are plotted as mean ± SEM *P < 0.05.

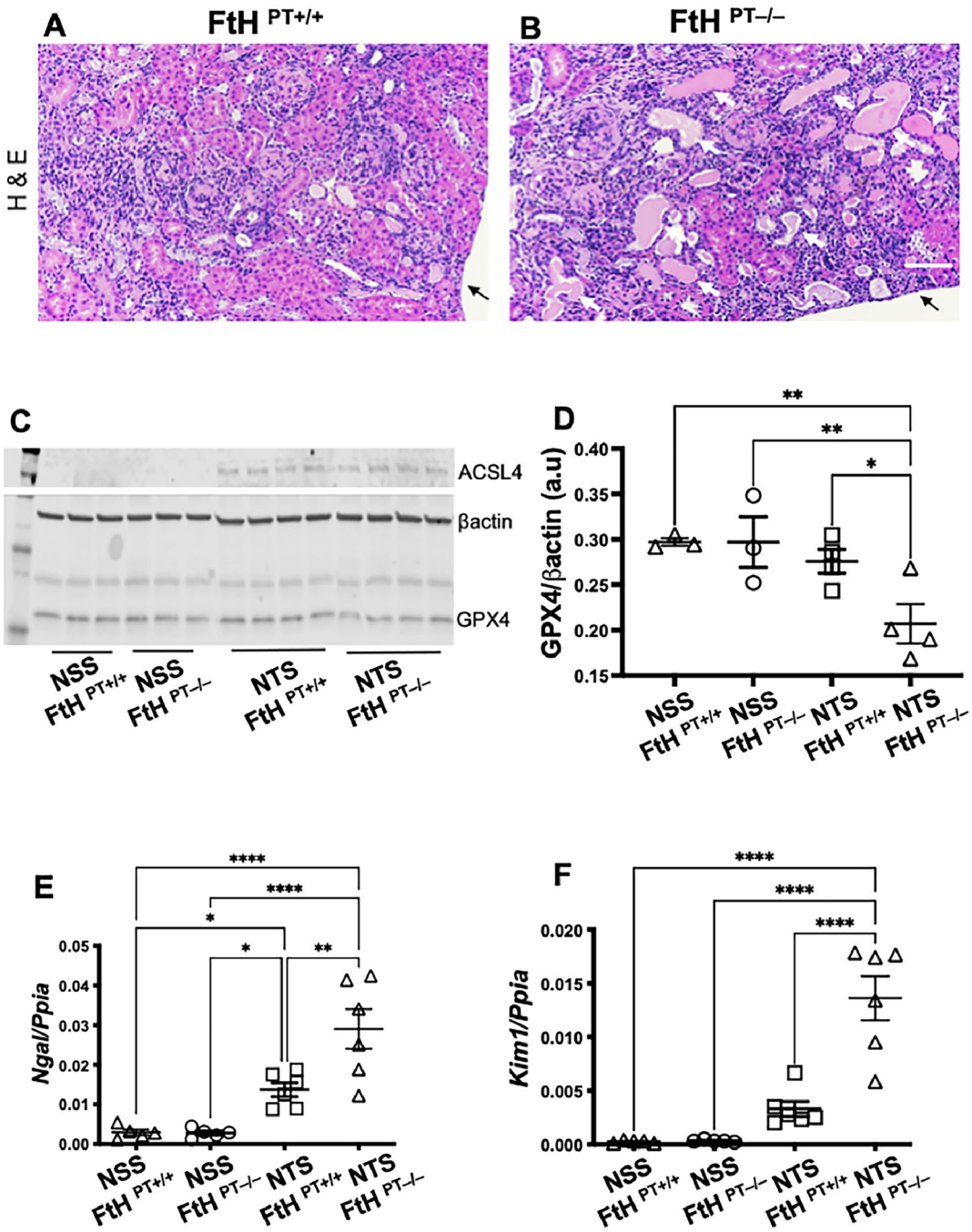

Figure 6. Loss of FtH1 in proximal renal tubules exacerbates ferroptosis and is associated with elevated tubular injury following glomerulonephritis.

12-week-old female $FtH^{PT-/-}$ or $FtH^{PT-/+}$ mice, were pre-sensitized with CFA (100ug), and four days later were injected i.v., with 100 uL normal sheep serum (NSS) or nephrotoxic sheep serum (NTS). Kidneys were analyzed 14 days later. Hematoxylin and Eosin (H&E) staining revealed inflammatory infiltrates in both the groups (A-B). However, compared to nephrotoxic serum injected $FtH^{PT+/+}$ mice (litter mate controls), $FtH^{PT-/-}$ mice had more tubular epithelial cell necrosis (dark pink fragmented cytoplasm with no nuclei) and denudation of the basement membrane (white arrows). Tubular casts, dilatation, luminal

debris were also obvious in the $FtH^{PT-/-}$ (B) Arrow denotes end of the section. Scale bar = 100 uM. Normal sheep serum immunization did not elicit changes in ACSL4 and GPX4 in both $FtH^{PT+/+}$ and $FtH^{PT-/-}$ mice (C-D). ACSL4 was upregulated comparably in nephrotoxic serum injected $FtH^{PT+/+}$ and $FtH^{PT-/-}$ mice (C-D). However, GPX4 expression was lowest in the nephrotoxic serum injected $FtH^{PT-/-}$. The observed renal pathology and exacerbated ferroptosis was supported by increased expression of proximal tubular injury markers *Ngal* (E) and *Kim1* (F) in $FtH^{PT-/-}$ mice.

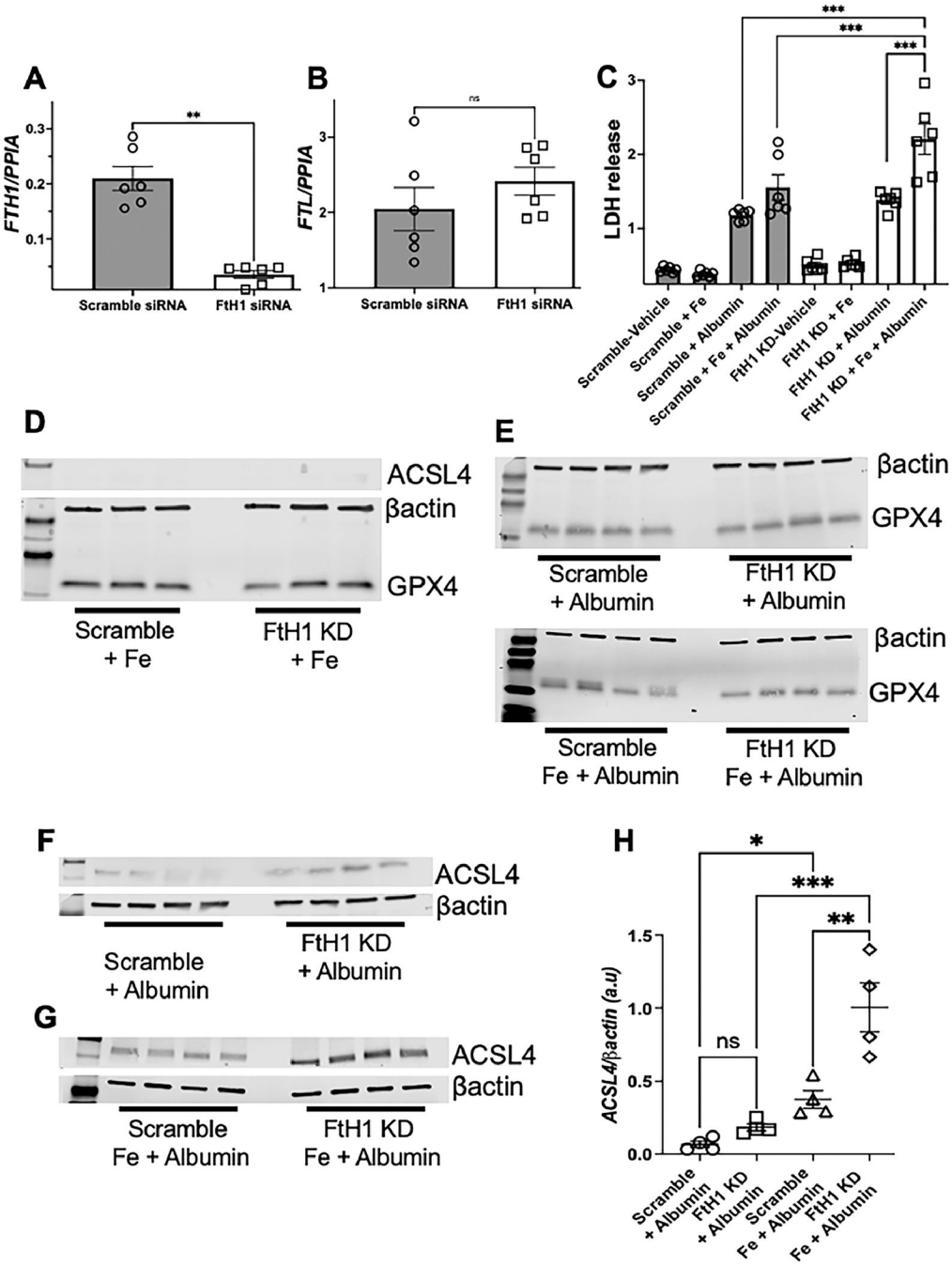

Figure 7. Combination of excess iron and protein overload exacerbates ferroptosis and cell death in FtH deficient human proximal renal tubular cells.

$2X10^5$ HK-2 cells (human proximal renal tubular cells) were treated with scramble siRNA or siRNA to H-ferritin which resulted in ~ 83% knockdown of H-ferritin gene (*FtH1*) (A). The ferritin light chain (*FtL*) was not affected (B). Following knockdown (83% after 52 h), cells were treated with vehicle, Ferrous sulphate (200 μg/mL), or human albumin (20 mg/mL) and the supernatants were analyzed for LDH levels after 12 h. Vehicle and Fe treated medium had comparable level of LDH in scramble or *FtH1* knock down (*FtH1* KD) groups (C). Albumin significantly but comparable induced cell death in both groups.

However, concomitant treatment with Fe and albumin significantly increased in cell death in FtH1 KD HK-2 cells (C). The involvement of ferroptosis in these conditions was evaluated by measuring the protein expression of ACSL4 and GPX4. Addition of iron did not induce ferroptosis in *FtH1* sufficient or knockdown cells (D). Albumin comparably reduced the expression of GPX4 (E) in scramble and *FtH1* KD cells, but increased the expression of ACSL4, which tended to be higher in the *FtH1* knockdown cells (F-H). Concomitant addition of Fe and albumin significantly increased ACSL4 expression in FtH1 sufficient cells, which was further elevated by FtH1 deficiency (G-H). Data was analyzed using 1-way and 2-way ANOVA with Holm-Šídák's multiple comparisons test and represented as mean ± SEM. **P < 0.001, ***P < 0.0001.

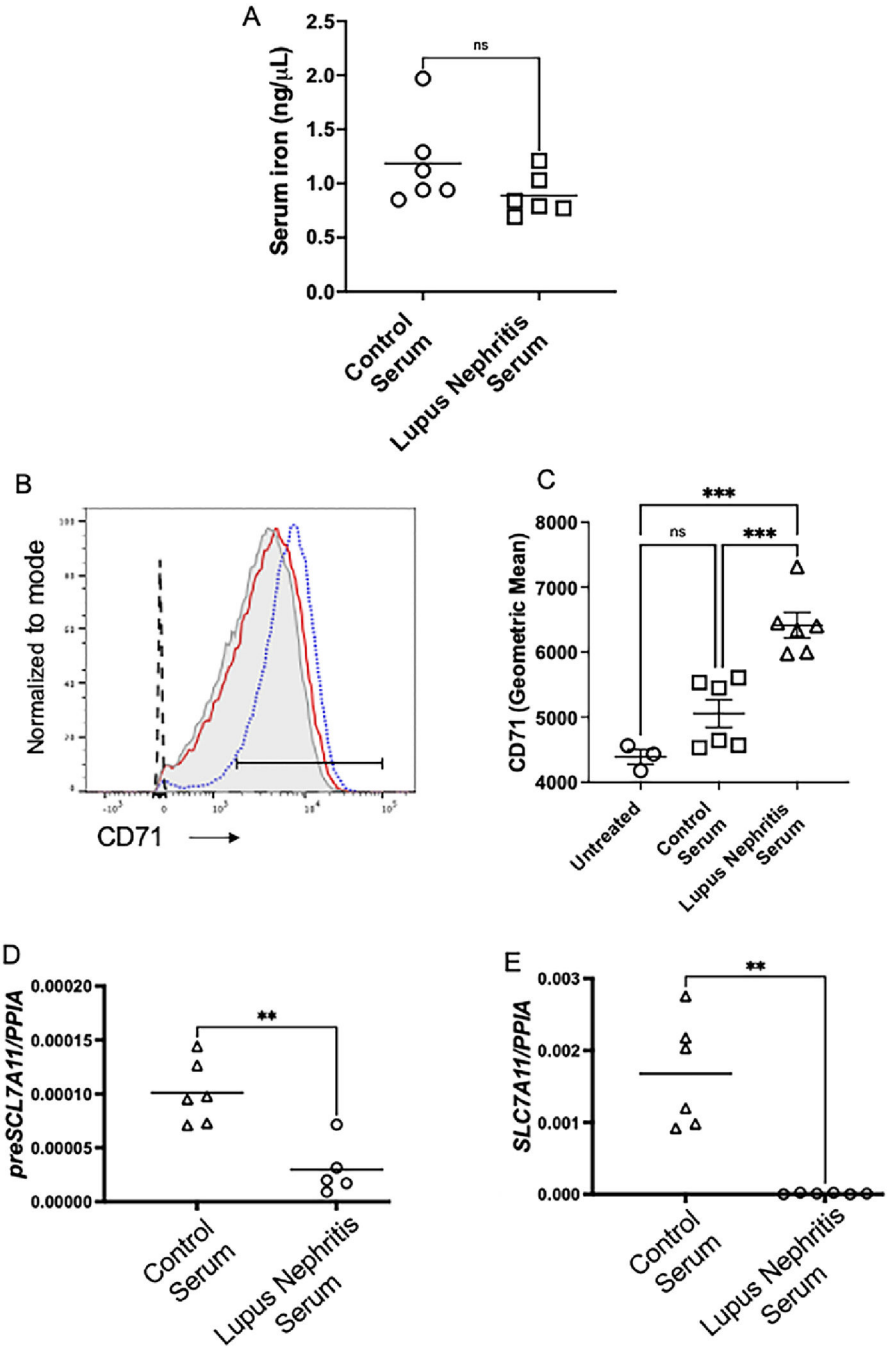

Figure 8. Lupus nephritis patients' serum activates iron uptake program and transcriptionally inhibits SLC7A11.

While the serum iron was comparable between normal donors and lupus nephritis patients (A), only lupus nephritis serum rapidly (30 min) and significantly increased CD71 (TfR1), a major iron uptake protein in human proximal tubular cell line (HK-2 cells) (B-C). Dotted black line: Unstained cells; Light grey filled histogram: tissue culture medium treated cells; Red line: normal donor serum treated cells; Blue dotted line: Lupus nephritis serum treated cells. Compared to healthy controls, lupus nephritis serum attenuated the expression of the precursor mRNA and gene expression of SLC7A11, indicating transcriptional inhibition.

Statistical significance was determined by 2-tailed Mann-Whitney test and using 2-way ANOVA with Tukey`s multiple comparison test. Only significant values are showed for comparison. Each dot represents an individual donor. Data is presented as mean. *P < 0.05, **P < 0.001, *** < 0.0001.

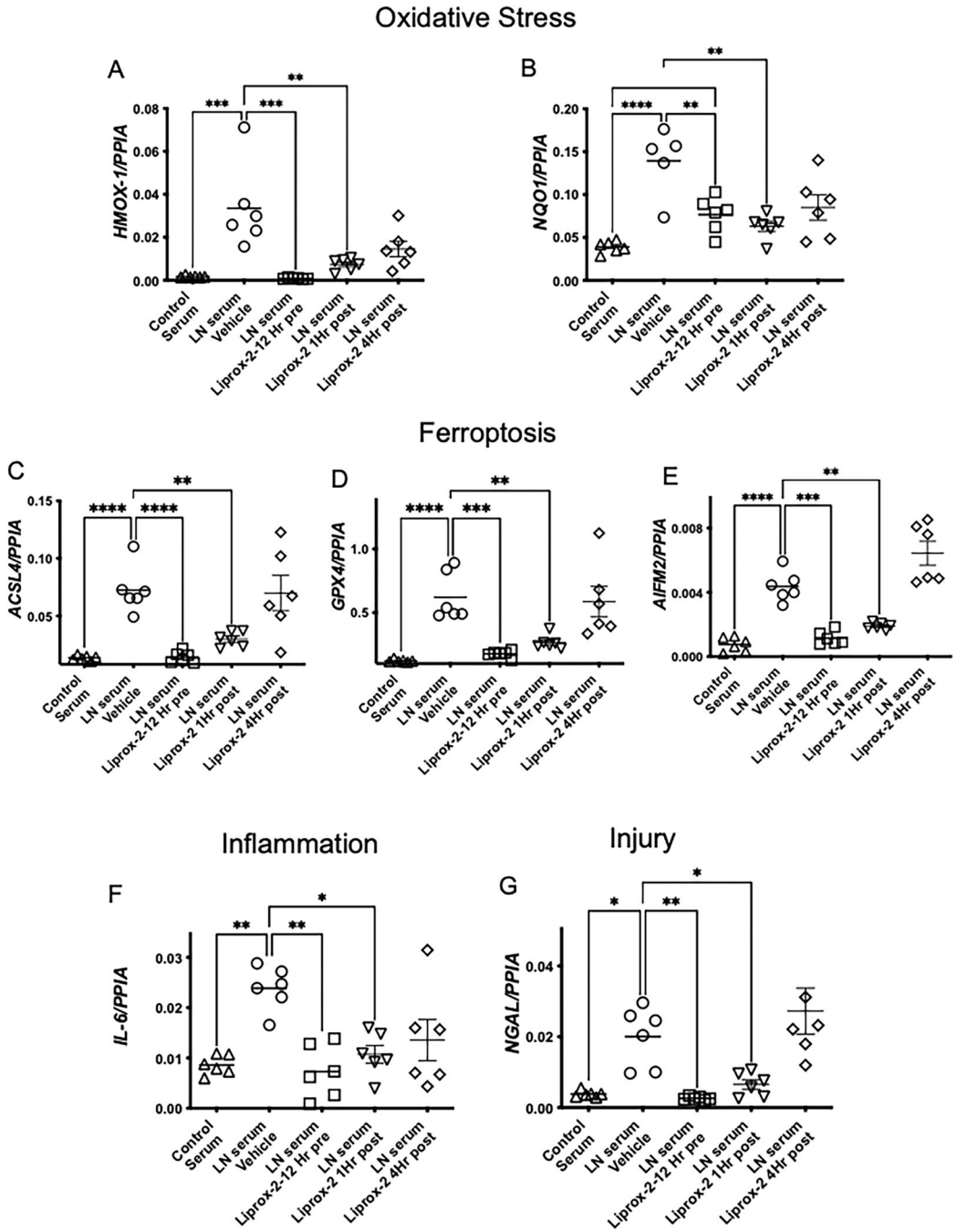

Figure 9. Lupus nephritis patients' serum induced ferroptosis in human proximal renal tubules, is mitigated by Liproxstatin-2, a novel ferroptosis inhibitor.

HK-2 cells were treated with vehicle (DMSO) or 100 nM Liproxstatin-2 for 12 h and then cultured with 5% normal control serum or serum from patients with class IV lupus nephritis. In some experiments Liproxstatin-2 was added 1 or 4 h after addition of the serum. All studies were terminated 24 h after serum addition. Compared to control serum, lupus nephritis serum induced a significant increase in gene expression of *HMOX-1*, *NQO1* (A-B) (Oxidative Stress), and *ACSL4*, *GPX4* and *AIFM2* (C-E) (Ferroptosis), *IL-6* (Inflammation) (F) and *NGAL* (injury) (G). All these pathological parameters were significantly reduced by

Liproxstatin-2 pretreatment or by adding it 1 hr after serum exposure. Lipoxstatin-2 did not have any benefit when added 4 h after exposure to lupus nephritis serum. Data was analyzed using 2-way ANOVA with Tukey`s multiple comparison test. Only significant values are showed for comparison. Each dot represents an individual donor. Data is presented as mean. *P < 0.05, **P < 0.001, *** < 0.0001.

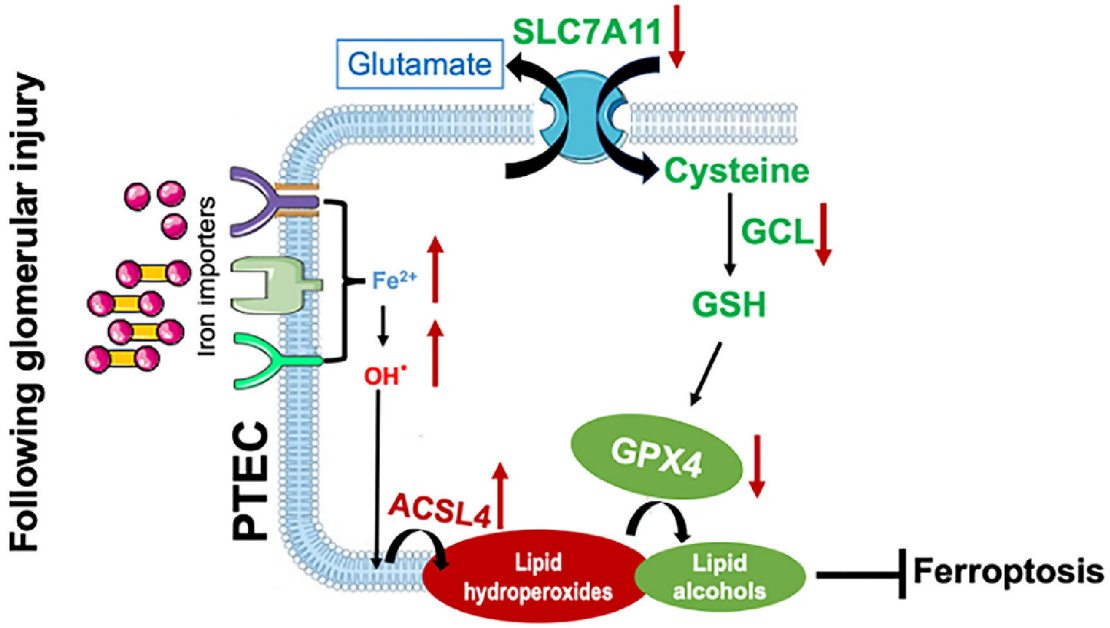

Figure 10. Proposed model of PTEC ferroptosis in lupus nephritis.

In normal physiological conditions little transferrin bound iron (TBI, red-yellow dumbbells) and non-transferrin bound iron (NTBI, red circles) is filtered by the glomerular assembly. This is reabsorbed and cycled by the proximal tubular cells (PTEC). However, in lupus nephritis, glomerular injury results in an increased leakage of TBI and NTBI, which can be reabsorbed by the PTEC via multiple receptors like TfR1, ZIP8/14 and megalin cubulin endocytic complex [34]. While TfR1 is regulated by the IRP-IRE system and can be downregulated by excess intracellular iron, ZIP8/14 and MCEC are not and continue to absorb the leaking TBI and NTBI to iron overload the PTEC [34]. This catalyzes the formation of free radicles and renders cells susceptible to ferroptosis. ACSL4 shapes the cellular lipid composition, which in presence of excess free radicles leads to the formation of toxic lipid hydroperoxides [43]. Attenuated expression of SLC7A11, impaired glutathione synthesis and the associated reduction in GPX4 hinder the conversion of toxic lipid hydroperoxides to nontoxic lipid alcohols and promote ferroptosis in lupus nephritis.